Apolipoprotein E associates with beta amyloid peptide of Alzheimer's disease to form novel monofibrils. Isoform apoE4 associates more efficiently than apoE3.

D A Sanan, … , B Frangione, A D Roses

Research Article

Late-onset and sporadic Alzheimer's disease are associated with the apolipoprotein E (apoE) type 4 allele expressing the protein isoform apoE4. Apolipoprotein E binds avidly to beta amyloid (A beta) peptide, a major component of senile plaque of Alzheimer's disease, in an isoform-specific manner. The apoE4 isoform binds to A beta peptide more rapidly than apoE3. We observed that soluble SDS-stable complexes of apoE3 or apoE4, formed by coincubation with A beta peptide, precipitated after several days of incubation at 37 degrees C with apoE4 complexes precipitating more rapidly than apoE3 complexes. A beta(1-28) and A beta(1-40) peptides were incubated in the presence or absence of apoE3, apoE4, or bovine serum albumin for 4 d at 37 degrees C (pH 7.3). Negative stain electron microscopy revealed that the A beta peptide alone self-assembled into twisted ribbons containing two or three strands but occasionally into multistranded sheets. The apoE/A beta coincubates yielded monofibrils 7 nm in diameter. ApoE4/A beta coincubates yielded a denser matrix of monofibrils than apoE3/A beta coincubates. Unlike purely monofibrillar apoE4/A beta coincubates, apoE3/A beta coincubates also contained double- and triple-stranded structures. Both apoE isoforms were shown by immunogold labeling to be uniformly distributed along the A beta peptide monofibrils. Monofibrils appeared earlier in apoE4/A beta than in apoE3/A beta in time-course experiments. Thus apoE3 and apoE4 each interact […]

Find the latest version:

https://jci.me/117407/pdf

Apolipoprotein E Associates with β Amyloid Peptide of Alzheimer's Disease to Form Novel Monofibrils

Isoform ApoE4 Associates More Efficiently Than ApoE3

David A. Sanan,* Karl H. Weisgraber,*[‡] Stephen J. Russell,* Robert W. Mahley,*[‡§] David Huang,[||] Ann Saunders,[||] Donald Schmechel,[||] Thomas Wisniewski,[¶] Blas Frangione,[¶] Allen D. Roses,[||] and Warren J. Strittmatter[||]

*Gladstone Institute of Cardiovascular Disease, Cardiovascular Research Institute, Departments of [‡]Pathology and [§]Medicine, University of California, San Francisco, California 94141-9100; [||]Departments of Medicine (Neurology) and Neurobiology, Joseph and Kathleen Bryan Alzheimer's Disease Research Center, Duke University Medical Center, Durham, North Carolina 27710; [¶]Department of Pathology, New York University Medical Center, New York 10016

Abstract

Late-onset and sporadic Alzheimer's disease are associated with the apolipoprotein E (apoE) type 4 allele expressing the protein isoform apoE4. Apolipoprotein E binds avidly to β amyloid (Aβ) peptide, a major component of senile plaque of Alzheimer's disease, in an isoform-specific manner. The apoE4 isoform binds to Aβ peptide more rapidly than apoE3. We observed that soluble SDS-stable complexes of apoE3 or apoE4, formed by coincubation with Aβ peptide, precipitated after several days of incubation at 37°C with apoE4 complexes precipitating more rapidly than apoE3 complexes. A$\beta_{(1-28)}$ and A$\beta_{(1-40)}$ peptides were incubated in the presence or absence of apoE3, apoE4, or bovine serum albumin for 4 d at 37°C (pH 7.3). Negative stain electron microscopy revealed that the Aβ peptide alone self-assembled into twisted ribbons containing two or three strands but occasionally into multistranded sheets. The apoE/Aβ coincubates yielded monofibrils 7 nm in diameter. ApoE4/Aβ coincubates yielded a denser matrix of monofibrils than apoE3/Aβ coincubates. Unlike purely monofibrillar apoE4/Aβ coincubates, apoE3/Aβ coincubates also contained double- and triple-stranded structures. Both apoE isoforms were shown by immunogold labeling to be uniformly distributed along the Aβ peptide monofibrils. Monofibrils appeared earlier in apoE4/Aβ than in apoE3/Aβ in time-course experiments. Thus apoE3 and apoE4 each interact with β amyloid peptide to form novel monofibrillar structures, apoE4 more avidly, a finding consistent with the biochemical and genetic association between apoE4 and Alzheimer's disease. (*J. Clin. Invest.* 1994. 94:860–869.) Key words: Alzheimer's disease • apolipoprotein E • electron microscopy • β amyloid peptide

Introduction

Alzheimer's disease (AD)[1] is a neurodegenerative disorder of the human brain culminating in memory loss and intellectual failure in late life (1). The clinical diagnostic criteria include progressive dementia with characteristic signs and symptoms, and the exclusion of other diseases that cause dementia. The neuropathologic criteria required for confirming the clinical diagnosis are the presence of senile or neuritic plaques, congophilic angiopathy, and neurofibrillary tangles in the cerebral tissue. The relationship between these neuropathologic structures, their numbers, location, and the disease mechanism is still unknown and controversial. The neuritic plaque and congophilic angiopathy have complex, incompletely characterized molecular and cellular constituents. Both extracellular structures contain aggregated Aβ peptide, a peptide of 39–43 amino acids produced by proteolytic cleavage of the amyloid precursor protein (APP) (for review, see Selkoe, 1991) (1). Aβ peptide forms β-pleated sheet fibrils that interact with Congo red dye or thioflavin silver stains to yield the definitive amyloid tinctural appearance of neuritic plaque. Other proteins present in the neuritic plaque and angiopathy include apolipoprotein E (apoE) (2–4), the APP itself, α-1–anti-chymotrypsin, IgG, several complement proteins, amyloid P, glycosaminoglycans (for review, see Beyreuther and Masters, 1991) (5), and SP 40, 40 (6). The molecular structure of fibrils occurring in the plaque and angiopathy, the mechanism of their assembly, and their role in the disease are unknown.

Recent genetic, biochemical, and histological investigations have demonstrated that apoE plays a critical role in Alzheimer's disease. Three isoforms of apoE—apoE2, apoE3 (the wild type), and apoE4—occur commonly in the human population and are the products of a gene located at chromosomal locus 19q13.2 (for review, see Mahley, 1988) (7). In the plasma, apoE plays a key role in targeting lipoproteins to cells involved in cholesterol and triglyceride metabolism. It serves as a major ligand for the LDL receptor (7). It also has been shown to be the main apolipoprotein synthesized in the brain (chiefly by astrocytes and macrophages/microglia) and is present in the cerebrospinal fluid as a component of lipoproteins and lipid complexes (8–

10). In addition, apoE is involved in peripheral nerve regeneration, redistributing lipids to axons during neurite extension and to Schwann cells during remyelinization (11–14). In the regenerating nerve, the expression of LDL receptors in the growing tips of axons and on the Schwann cells is coordinated with the secretion of apoE by macrophages. In vitro apoE in combination with cholesterol alters neurite outgrowth in dorsal root ganglia by decreasing branching and stimulating neurite elongation (15). Specifically, apoE3 stimulates neurite outgrowth, whereas apoE4 impairs neurite outgrowth (16).

The linkage of apoE, and specifically the apoE4 allele (apoE4), with the occurrence of late-onset familial (4) and sporadic AD (17) opens up a new area of investigation of the role of this protein in the nervous system. It now has been established that apoE4 is a major risk factor for late-onset AD, increasing the incidence and decreasing the age of onset as a function of the inherited dose of this allele (18). Moreover, patients homozygous for apoE4 almost always develop the disease by age 80 (18). Further, apoE has been immunolocalized in neuritic plaque and angiopathy (2). Patients homozygous for apoE4 have greatly increased $A\beta$ peptide immunoreactivity in senile plaques and congophilic angiopathy (19). In vitro apoE binds to $A\beta$ peptide with high avidity, forming a complex that is not dissociated by heating in sodium dodecyl sulfate. Two isoforms, apoE3 and apoE4, have different binding characteristics with $A\beta$: apoE4 binds more rapidly and over a narrower pH range than apoE3 (20). Of note, apoE binds to $A\beta$ within the region delimited by amino acids 12–28, the same region implicated in fibril formation (20).

These biochemical, pathologic, genetic, and epidemiologic associations of apoE with AD have stimulated the present morphological investigation of the interactions of the apoE3 and apoE4 isoforms with $A\beta$ peptide. We report here transmission electron microscopy studies that demonstrate in vitro that (*a*) apoE interacts with $A\beta$ peptide to produce a novel monofibrillar form that contains tightly bound apoE and (*b*) apoE4 does this more efficiently than apoE3. These findings support the view that apoE, and apoE4 in particular, may play a key role in the pathogenesis of AD.

Methods

The apoE3 and apoE4 isoforms were isolated from the plasma of fasting subjects with the apoE3/3 and apoE4/4 phenotypes, as described previously (21). Synthetic $A\beta$ peptides $A\beta_{(1-28)}$ and $A\beta_{(1-40)}$ were purchased from Bachem California (Torrance, CA). The lyophilized $A\beta$ peptide (1 mg) first was dissolved in 60 μl of distilled water before dilution with phosphate-buffered saline (PBS), pH 7.3, to the indicated concentrations. In some experiments, the $A\beta$ peptide was purified by fast performance liquid chromatography (FPLC) on a Superose 12 column (Pharmacia Fine Chemicals, Uppsala, Sweden) to generate a starting solution containing only $A\beta$ monomers. Bovine serum albumin (crystallized, A-7638), purchased from Sigma Chemical Co. (St. Louis, MO), was used to control for nonspecific protein effects on fibril function.

Coincubation experiments. Purified apoE3 (10 μg or 1.8 × 10^{-6} M), apoE4 (10 μg or 1.8 × 10^{-6} M), or bovine serum albumin (10 μg) was incubated at 37°C for 4 d with $A\beta$ peptide (100 μg or 2.5 × 10^{-4} M) in 100 μl PBS. This ratio of apoE to $A\beta$ is derived from biochemical studies previously described in which these concentrations and ratios were determined to be optima for the formation of the apoE/$A\beta$ peptide complex (20). The pH optima for formation of the apoE/$A\beta$ peptide complex also were previously shown to lie between 7.0 and 7.6 (20).

For this reason the physiological pH of 7.3 was used in the present studies. Optimal concentrations of $A\beta$ peptide for ribbon formation in vitro were determined experimentally to be 1–2 mg/ml. Both isoforms of apoE also were incubated alone as controls. In some experiments, β-mercaptoethanol (1% final concentration) was included in the incubation mixture to create reducing conditions. For polyacrylamide gel electrophoresis (PAGE), incubations were stopped by the addition of 10 μl of 2× Laemmli buffer (4% SDS, no β-mercaptoethanol) to 10-μl aliquots and heated at 100°C for 5 min. Proteins were electrophoresed on 12% polyacrylamide gels containing 2% SDS and then transferred to Immobilon P membranes (Millipore Corp., Bedford, MA). The membranes were washed and incubated in rabbit anti-$A\beta$ peptide antibody (Boehringer Mannheim Biochemicals, Indianapolis, IN) at 1:80 overnight, then with horseradish peroxidase conjugated secondary antibody, and chemiluminescence (enhanced chemiluminescence kit, Amersham Corp., Arlington Heights, IL) was visualized by exposure to Hyperfilm (Amersham Corp.).

Time-course studies. Incubations of $A\beta$ alone, and with apoE3 or apoE4, were conducted over a 7-d time-course. Aliquots were removed for SDS-PAGE daily for 4 d, and for electron microscopy at the start and after 1, 4, and 7 d to monitor ribbon and monofibril appearance. Since ribbons were observed in $A\beta$ peptide freshly dissolved from lyophilized material, solutions were passed through an FPLC column to ensure that only $A\beta$ monomers were present at the start of the time-course experiments.

Negative staining electron microscopy. At the end of the incubations, 5-μl aliquots were placed on carbon-filmed 400 mesh grids for 30 s, drawn off with the torn edge of a piece of Whatman No. 1 filter paper, and negatively stained with 2% aqueous silicotungstic acid (19431: Ted Pella, Inc., Tustin, CA) containing 0.1% sucrose, pH 7.0. Grids were examined at 80 kV in a JEM 100CXII transmission electron microscope (JEOL Ltd., Tokyo, Japan). The nominal instrument magnifications were corrected using a silicon monoxide grating replica with 54,863 lines/inch (Ernest Fullam, Inc., Latham, NY) as a calibration standard. Dimensional measurements were made directly from prints using a 15× scale loupe graduated in tenths of a millimeter. All electron microscopy was performed with a liquid nitrogen–cooled anticontamination device in operation.

Immunogold techniques. The position of apoE on the filaments generated during incubations was determined by on-grid immunogold labeling. All steps were conducted at room temperature unless otherwise specified. Preparations were washed twice in 10 vol of PBS by centrifugation at 16,000 *g* in a microfuge for 15 min to remove unbound apoE3 or apoE4. Carbon-filmed 400 mesh copper/palladium grids were floated film side down on droplets of 41-kD polylysine (P2636, Sigma Chemical Co.) at 0.5 mg/ml in reagent-grade deionized water for 5 min. The grids were dried with Whatman No. 1 filter paper and then floated on the undiluted $A\beta$ peptide and apoE coincubate samples for 5 min. Grids were washed in PBS for 2 min, blocked in 3% bovine serum albumin (A-2153, Sigma Chemical Co.) in PBS for 1 h, washed in Tris-buffered saline (TBS) (20 mM Tris-HCl, 225 mM NaCl, 5 mM sodium azide, pH 8.0) for 1 min, and incubated with antibodies for 1 h at room temperature. Monoclonal antibodies (gifts from Dr. Ross Milne, University of Ottawa Heart Institute, Ottawa Civic Hospital) were used to immunolocalize apoE: antibodies designated 3H1 were directed against the carboxyl-terminal region of apoE, 6H7 against the amino terminus, and 1D7 against the receptor-binding region of the protein (residues 140–150). Antibodies were diluted 1:500 (vol/vol) in TBS containing 0.1% ovalbumin (A-5503: Sigma Chemical Co.) and were incubated for 1 h with the specimen grids. Normal mouse serum (M-5905: Sigma Chemical Co.) diluted 1:500 (vol/vol) was used as a control for nonspecific binding of the primary antibodies. Following the antibody incubations, the specimens were rinsed four times, for 5 min each, with 0.1% ovalbumin-TBS, and then incubated with goat anti-mouse IgG conjugated with colloidal gold particles 10 nm in diameter (49-6503: Zymed Labs., Inc., South San Francisco, CA) diluted 1:50 (vol/vol) in 0.1% ovalbumin-TBS. After exhaustive washing with 0.1% ovalbumin-TBS, grids were jet-washed for 15 s in a stream
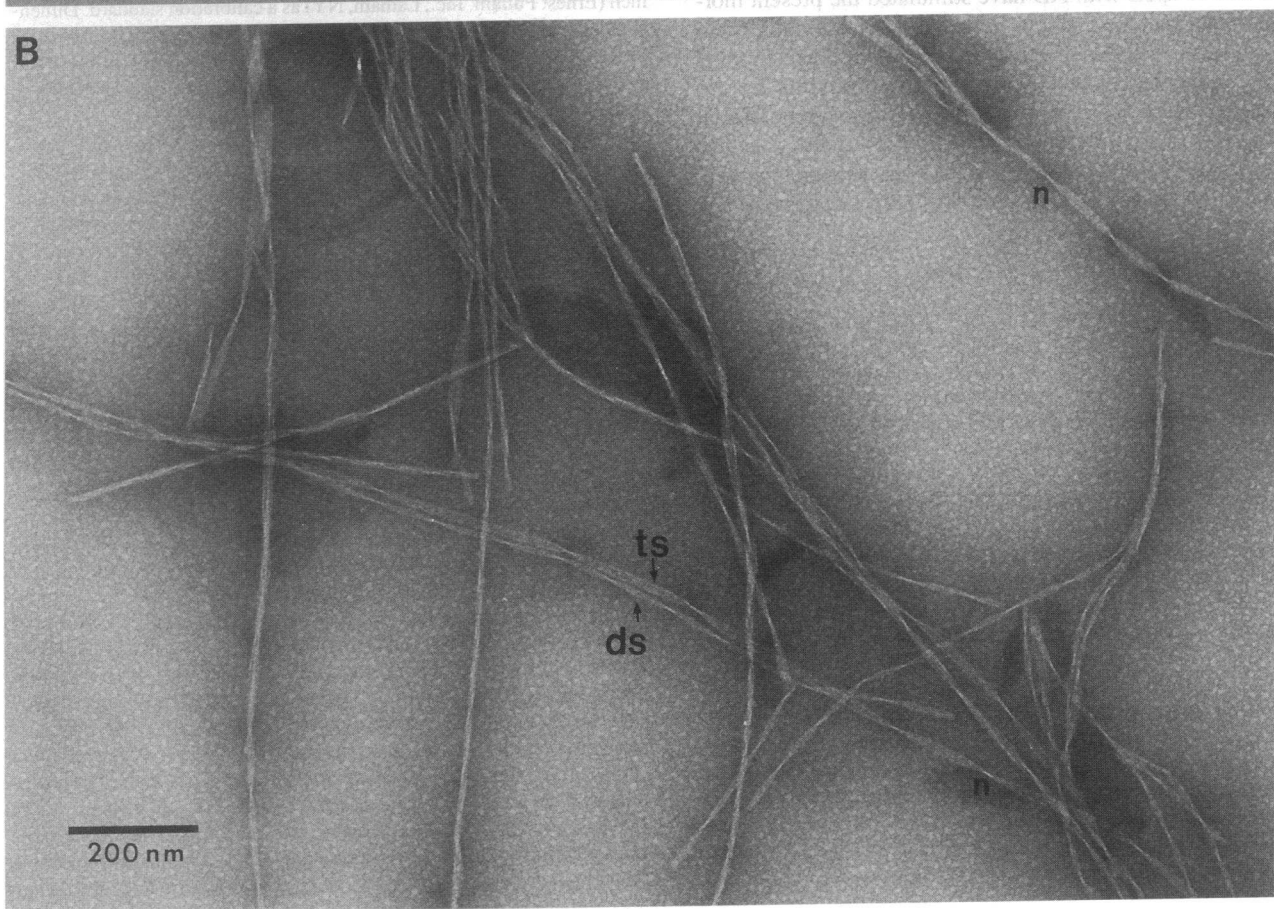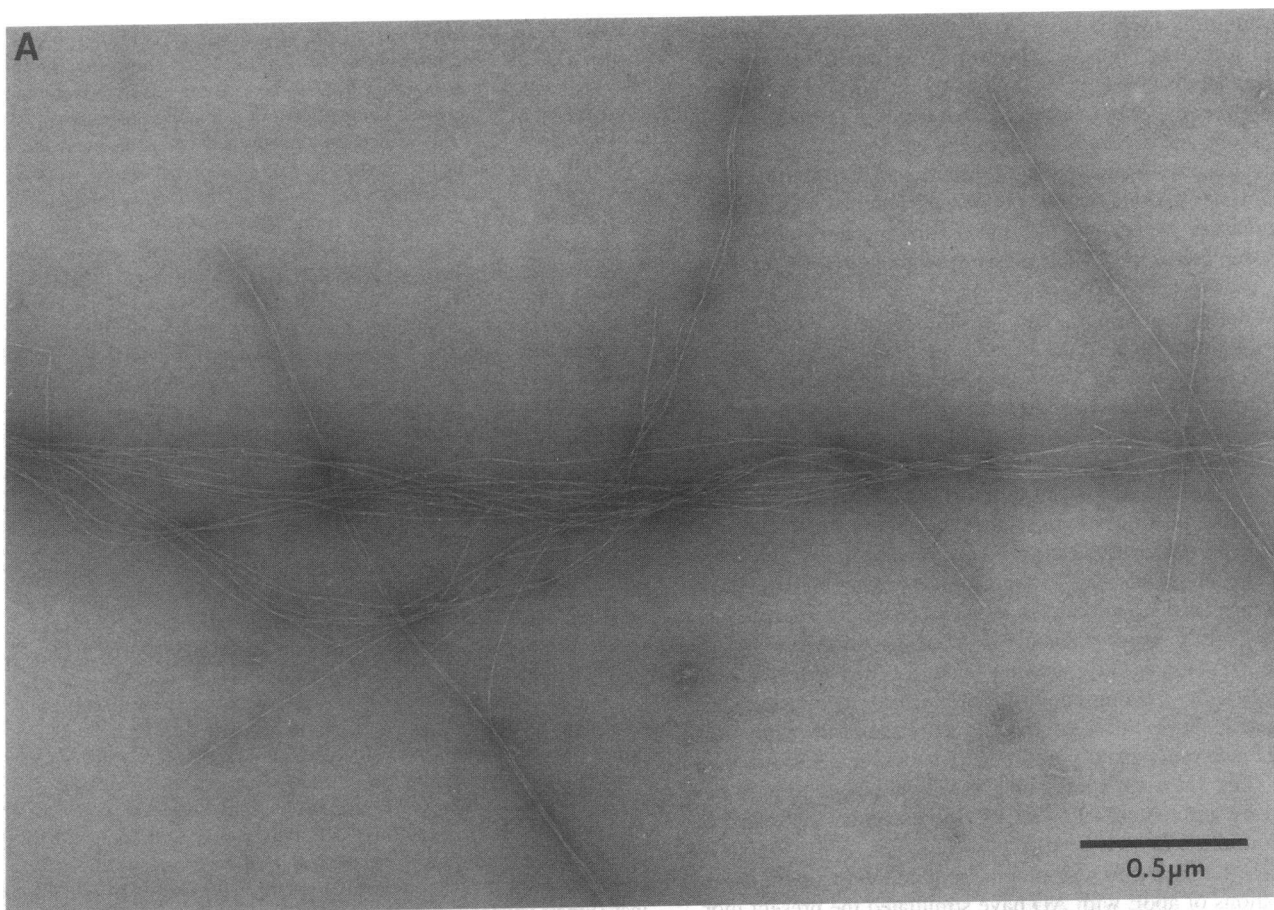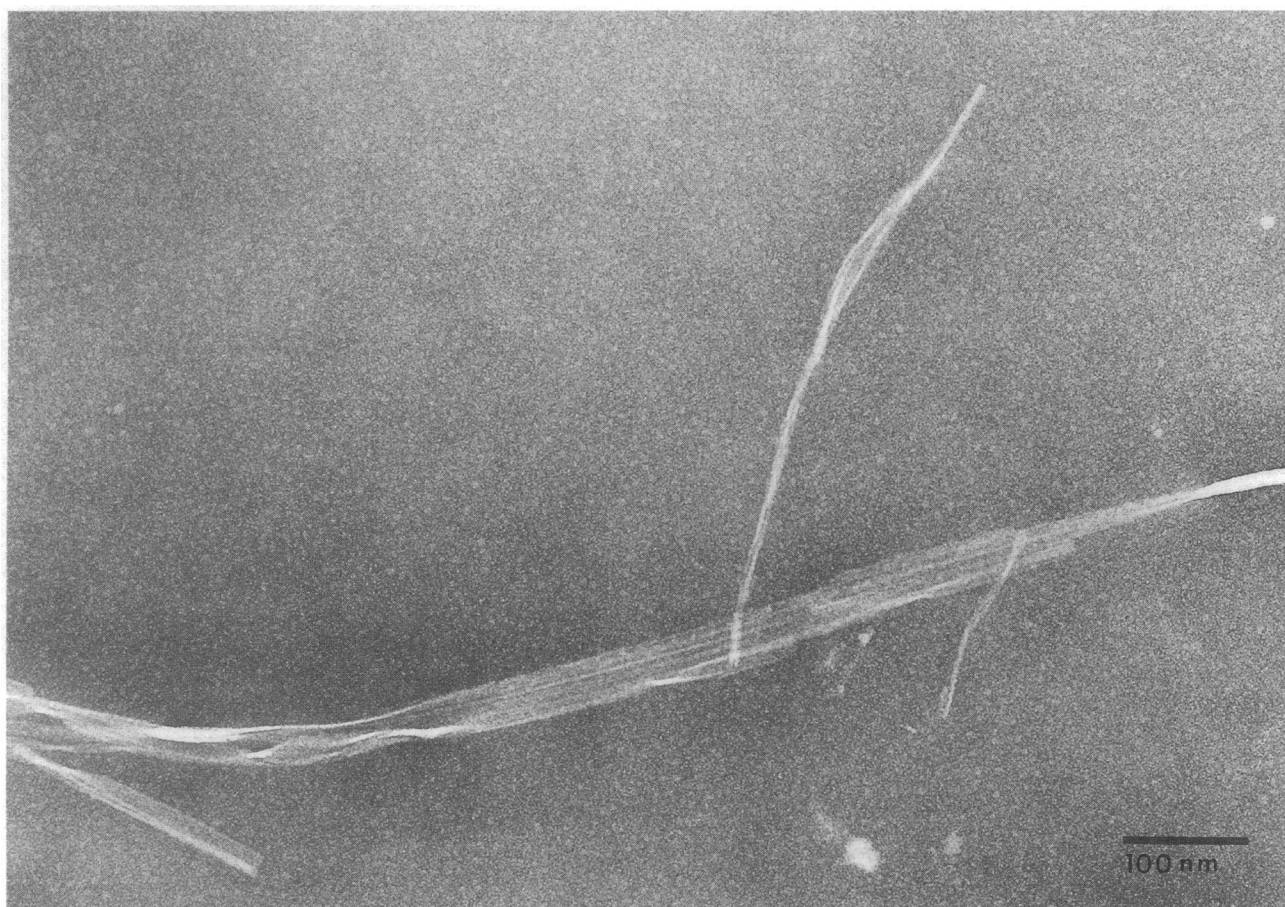
Figure 2. Sheet formation by Aβ peptide. Preparation was exactly as for specimens in Fig. 1. High-power view of a multistranded, sheet-like portion of an Aβ ribbon. ×126,170. Bar, 100 nm.

of reagent-grade deionized water, air dried, and negatively stained with 2% silicotungstic acid. The grids were examined in a transmission electron microscope as described above.

Congo red staining. The Aβ peptide (1 mg/ml), alone and coincubated with apoE3, apoE4, or bovine serum albumin (100 μg/ml in distilled water), was spotted (20-μl aliquots) onto gelatin-coated glass microscope slides and air dried at 37°C. Slides then were immersed in 0.2% Congo red (C-6277: Sigma Chemical Co.) dissolved in 80% aqueous ethanol saturated with NaCl (pH 10.5–11.0) for 60 min at room temperature (22). Slides were washed three times with distilled water, dried, and examined by polarized light microscopy.

Results

We determined that $A\beta_{(1-28)}$ incubated alone for 4 d at 37°C in PBS produced twisted ribbon-like filaments observed by negative staining electron microscopy (Figs. 1 *A* and *B*, and 2). (We will henceforth refer to the twisted ribbon-like filaments simply as ribbons.) Most of the observed ribbons had two clear, longitu-

dinal striations that made them appear double-stranded (Fig. 1 *B*). The average width of the double-stranded ribbons was 14 ± 1 nm. Triple-stranded ribbons (average width 19 ± 2 nm) also were seen, but not as frequently as double-stranded forms (Fig. 2). The ribbons were twisted randomly, as the nodes were aperiodic (Fig. 1 *B*). It was possible to estimate the thickness of the ribbons as ~ 10 nm by measuring them at the nodes, where they are imaged edge-on (Fig. 1 *B*). The Aβ peptide ribbons were all relatively long (well in excess of 2 μm in Fig. 1 *A*), unbranched, truncated at the ends, and twisted into skeins or bundles (Fig. 1 *A*). Occasionally, Aβ ribbons were multistranded and very wide, resembling sheets; a wide ribbon (~ 60 nm across) composed of at least five strands is shown in Fig. 2.

To rule out the possibility that the double- and triple-stranded ribbons and multistranded sheets might be artifacts of staining, we made 10- and 100-fold dilutions of Aβ peptide incubations just prior to negative staining electron microscopy.

Figure 1. Twisted ribbons formed by Aβ peptide. Aβ peptide was freshly dissolved from lyophilized material and incubated for 4 d at 37°C at 1 mg/ml in phosphate-buffered saline, pH 7.3. Samples were negatively stained in 2% silicotungstic acid, pH 7.0. (*A*) Low-power view of bundles of Aβ ribbons. Note that most ribbons in the field are 2 μm or greater in length. ×44,900. Bar, 0.5 μm. (*B*) Twisted Aβ ribbons of two different widths: double-stranded (ds) and triple-stranded (ts). Note twist nodes (n). ×89,600. Bar, 200 nm.
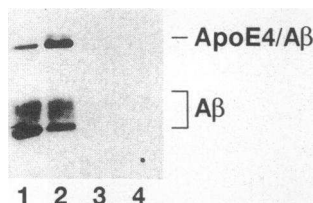
In these dilutions we found Aβ ribbons of all three types, whose formation would have been extremely unlikely under high dilution conditions.

We observed that when Aβ$_{(1-28)}$ peptide was coincubated with apoE4 for 4 d, there was a complete loss of the SDS-soluble Aβ/apoE4 complex from the solution after 2 d, as determined by polyacrylamide gel electrophoresis (Fig. 3). In the case of apoE3, the complex persisted for 4 d (not shown). The loss of apoE4/Aβ complex strongly suggested the formation of a precipitate or SDS-insoluble aggregate. When 4-d, 37°C coincubates of Aβ$_{(1-28)}$ and apoE4 were examined by negative staining electron microscopy, a novel fibrillar matrix was observed (Fig. 4). Monofibrils, 7 nm at the widest and ranging in length from 75 nm to 2 μm, were seen. The qualitative differences between these monofibrils and pure Aβ ribbons can be appreciated by comparing them as shown in Fig. 4 and Fig. 1 *B*, respectively. Monofibrils of Aβ/apoE4 were hardly ever seen running parallel to one another. Similar monofibrils (up to 1 μm in length) were observed when Aβ$_{(1-40)}$, a peptide species commonly found in AD plaques, was incubated with apoE4 (not shown).

Incubation of apoE3 with Aβ peptide led to the formation of monofibrils, but fewer than in apoE4/Aβ coincubates (Fig. 5 compares undiluted samples directly from the incubation mixtures). The most striking result of the apoE4 interaction with Aβ peptide was the production of a dense, matrix-like meshwork of 7-nm monofibrils (Fig. 5 *A*). In the same time period, apoE3 produced a much less dense matrix (Fig. 5 *B*). Equivalent quantities of apoE were used in the incubations in each case, so the reduced number of fibrils may reflect a lower potency of apoE3 to generate monofibrils with Aβ. In addition, residual Aβ ribbons, both double-stranded and triple-stranded, were found in apoE3/Aβ coincubates (Fig. 5 *B*), while apoE4/Aβ coincubates were devoid of them (Fig. 5 *A*). In some coincubation experi-
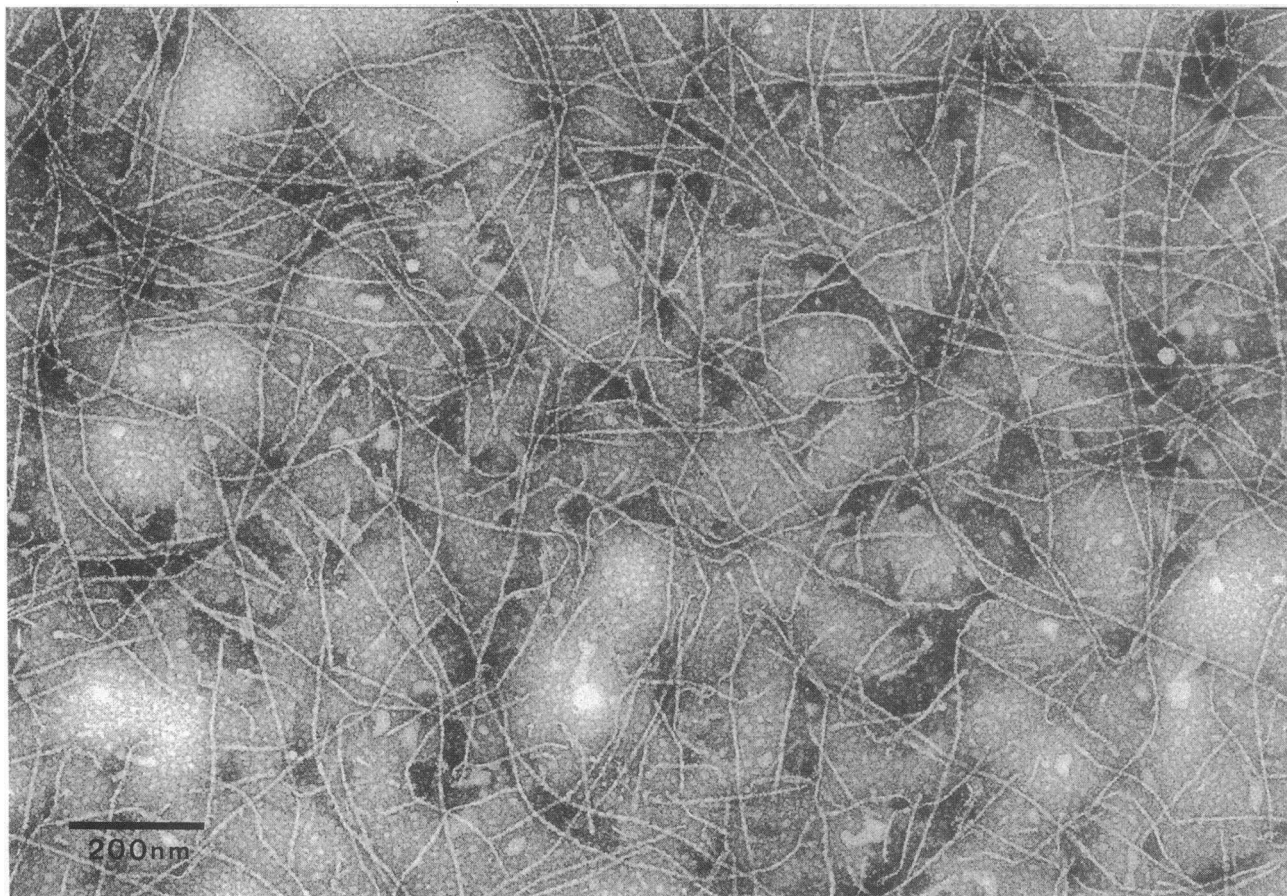
*Figure 4.* Morphology of monofibrils generated upon coincubation of apoE4 with Aβ peptide. Aβ peptide was freshly dissolved from lyophilized stock in phosphate-buffered saline (pH 7.3) at 1 mg/ml and incubated with apoE4 at 1 mg/ml for 4 d at 37°C. Negative stains were made with 2% silicotungstic acid. ×89,600. Bar, 200 nm. Monofibrils (6–7 nm) were generated when apoE4 and Aβ peptide were coincubated.
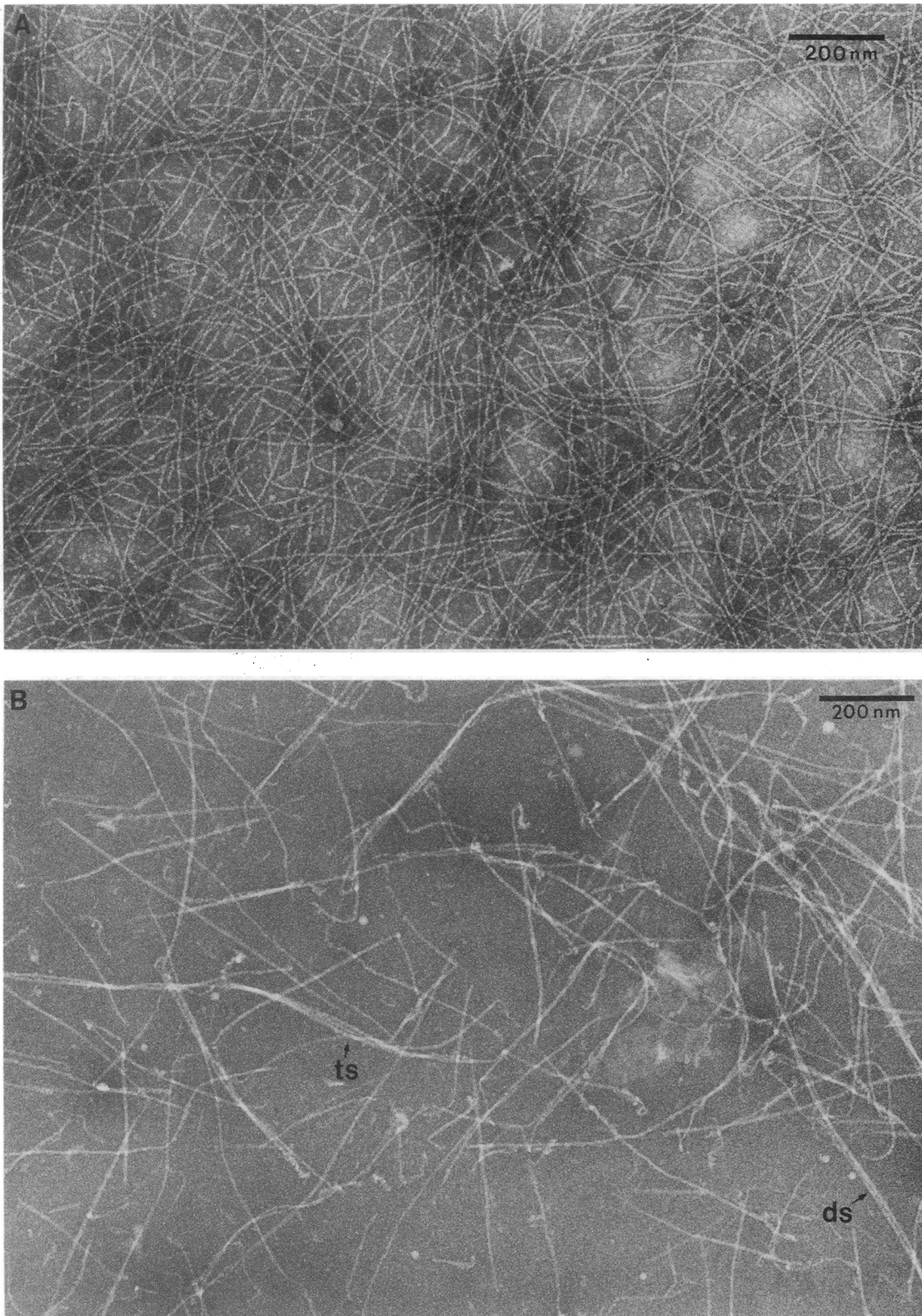
Figure 5. Comparison of monofibrils generated by coincubations of apoE4 or apoE3 with Aβ peptide. The monofibrils were produced and negatively stained as described in the legend for Fig. 3. 4-d coincubates are pictured. (*A, B*) ×89,600. Bar, 200 nm. (*A*) Very dense apoE4/Aβ monofibril matrix devoid of double- or triple-stranded Aβ ribbons. (*B*) Less dense apoE3/Aβ matrix consisting mainly of monofilaments but with residual double-stranded (ds) and triple-stranded (ts) ribbons, the strands of which are slightly separated.
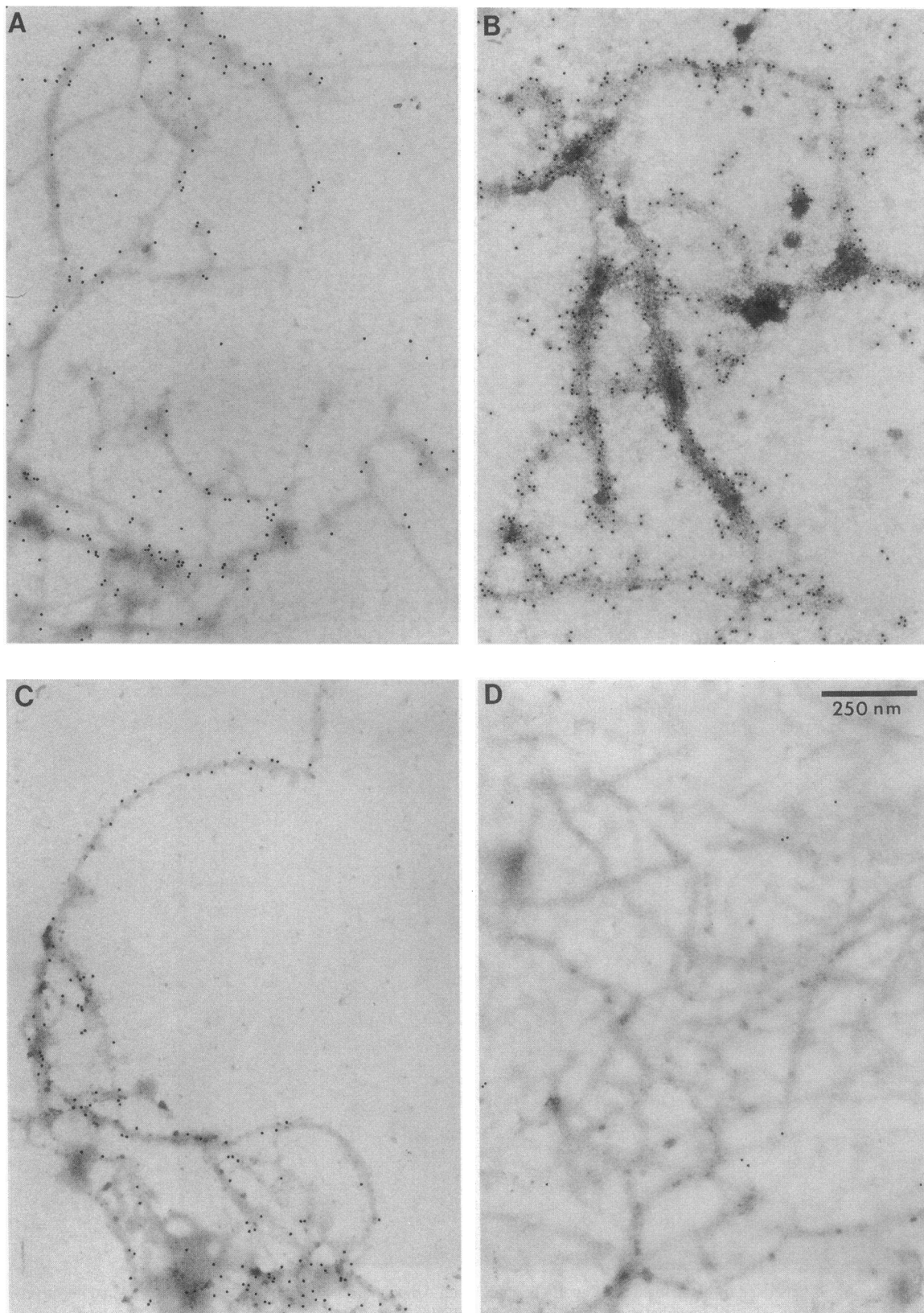
Figure 6. Immunogold labeling of apoE in monofibrils generated in coincubates of apoE4 with Aβ peptide. Monofibrils were produced as described in the legend for Fig. 3. Monofibrils were exhaustively washed with PBS to remove free apoE, mounted on poly-*l*-lysine–coated grids, and then incubated with control serum or monoclonal antibodies against apoE, which in turn were detected by immunogold staining with goat anti-mouse IgG conjugated with 10 nm colloidal gold particles. The background levels of gold binding were extremely low. ×51,170. Bar, 250 nm. (*A*) ApoE4/

ments, bovine serum albumin was used instead of apoE to control for nonspecific protein effects on $A\beta$ ribbon formation. In these coincubates, only twisted ribbons, like those produced by $A\beta$ alone, were seen (not shown).

Immunogold labeling of apoE associated with fibrils. The location of both apoE3 and apoE4 on (or in) the monofibrils from apoE/$A\beta$ coincubations was detected by immunogold labeling. Three monoclonal antibodies (3H1, 1D7, and 6H7) were used to detect apoE. In each case, the monoclonal antibody against apoE bound along the entire length of the fibril, indicating that apoE was either adsorbed to, or incorporated within, the fibril (Fig. 6 $A-C$). The fibrils were not immunoreactive to control IgG from normal mouse serum (Fig. 6 D). In every case, background gold labeling was extremely low. The apoE3 and apoE4 control grids were heavily immunoreactive with apoE antibodies (not shown), but not with control IgG from normal mouse serum.

Immunostained specimens of apoE4/$A\beta$ monofibrils were adsorbed to poly-l-lysine–coated carbon-filmed grids. In these preparations (Fig. 6 $A-D$), the monofibril distribution appeared different from that seen in negative stains on grids that were not treated with poly-l-lysine (Fig. 4). In the latter case, single monofibrils of apoE4/$A\beta$ complexes were seen. On poly-l-lysine substrata the monofibrils tended to align in parallel (Fig. 6 B), but these were distinctly different from $A\beta$ ribbons (Fig. 1).

Previous experiments demonstrated that binding of $A\beta$ peptide by apoE was abolished by β-mercaptoethanol (20). Therefore, the effects of the reducing agent on monofibril formation were examined at the electron microscope level. Coincubations of $A\beta$ peptide with apoE3 or apoE4 in the presence of 1% β-mercaptoethanol produced only twisted ribbons, similar to those produced from $A\beta$ peptide alone. The mechanism of the β-mercaptoethanol effect is unclear, but the effect itself is consistent with biochemical data (20). Monofibrils were not observed in the presence of β-mercaptoethanol (not shown).

Time-course studies. Incubations of $A\beta$ alone and with apoE3 or apoE4 were run for 7 d. The purified $A\beta$ peptide incubated alone produced a few short ribbons of the order of 250 nm in length by day 1, longer ones (in excess of 2 μm) by day 4, and by day 7 multistranded sheets were seen. The fact that ribbons became longer and multistranded with increasing incubation time clearly shows that these morphological forms of the $A\beta$ peptide were not artifactually generated during negative staining. In apoE4/$A\beta$ coincubates, short monofibrils were first observed on day 4. By day 7 these monofibrils were longer and more numerous. No $A\beta$ ribbons were present on days 4 or 7 in the presence of apoE4. In contrast, apoE3/$A\beta$ coincubates produced very few short fibrils throughout the time-course. The most strikingly different feature of the apoE3/$A\beta$ coincubates was the presence of double-stranded $A\beta$ ribbons in the day 7 samples.

Congo red staining. The $A\beta$, apoE3/$A\beta$, and apoE4/$A\beta$ preparations stained with Congo red demonstrated a greenish

birefringence characteristic of amyloid peptides when observed by polarized light microscopy. The bovine serum albumin preparation was stained similarly but showed no birefringence.

Discussion

We have shown here by electron microscopy that $A\beta_{(1\text{-}28)}$ or $A\beta_{(1\text{-}40)}$ peptides interact with both apoE3 and apoE4 to produce monofibrils of a morphology distinct from that of the multi-stranded, twisted ribbons formed by $A\beta$ alone. Uniquely, however, the apoE4 isoform interacts more efficiently with $A\beta$ to produce a more complex meshwork of monofilaments than that observed with apoE3. Apolipoprotein E was clearly immunolocalized on or in these monofibrils by the specific binding of three different monoclonal antibodies, each specific for a different region of apoE. The full length of the monofibrils was uniformly labeled, suggesting that apoE may have been adsorbed to the surface of the monofibrils or even intercalated between the $A\beta$ monomers, perhaps forming a novel hybrid fibril. The width of the monofibrils is between 6 and 7 nm, which is the same order of magnitude reported for amyloid fibrils produced in vitro (22–25). Our morphological findings are consistent with recent biochemical data on the interaction of $A\beta$ peptides and apoE. High-avidity interactions between apoE and $A\beta$ peptides recently have been characterized, with amino acids 12–28 of $A\beta$ peptide required to bind apoE (4). The resultant complex is extremely stable, resisting dissociation by heating in sodium dodecyl sulfate. Moreover, the binding affinity of $A\beta$ for apoE is isoform specific, with apoE4 forming complexes more rapidly than apoE3 (20). It has already been reported that when coincubates of the 22-kD receptor-binding amino-terminal fragment of apoE and the $A\beta$ peptide were analyzed by PAGE, complexes were not found (20). For this reason we did not study such coincubates by electron microscopy.

We have presented here morphological evidence consistent with apoE3 and apoE4 isoform-specific effects: apoE4 induced the formation of a denser monofibrillar matrix than apoE3 in a given time period. In the presence of apoE4, much longer monofibrils are formed, and there is a complete absence of $A\beta$ ribbons. In the presence of apoE3, less dense and shorter monofibrils are formed, and $A\beta$ ribbons remain. Previous biochemical studies demonstrated that the reducing agent β-mercaptoethanol prevented interactions of $A\beta$ and apoE (20). Our current morphologic studies demonstrated that β-mercaptoethanol also completely abolished the ability of apoE and $A\beta$ to form monofibrils and are thus completely consistent with biochemical findings. Bovine serum albumin was used to control for nonspecific effects of apoE that might cause $A\beta$ peptide to form monofibrils. Albumin was chosen because it is likely to be present at the sites of senile plaque formation in vivo. In the presence of bovine serum albumin, $A\beta$ formed twisted ribbons identical to those formed by $A\beta$ alone. Thus, at the biochemical and morphologic levels, the effects of apoE3 and apoE4 on $A\beta$

$A\beta$ coincubate monofibrils labeled with monoclonal antibody 3H1. Gold particles decorate the fibrils along their lengths. (*B*) ApoE4/$A\beta$ coincubate monofibrils labeled with monoclonal antibody 1D7. The fibrils are in bundles that are heavily labeled with gold. (*C*) ApoE4/$A\beta$ coincubate fibrils labeled with monoclonal antibody 6H7. Gold particles delineate the fibrils uniformly. (*D*) ApoE4/$A\beta$ coincubate monofibrils labeled with normal mouse IgG as a negative control for the primary antibody. The gold particle background is very low.

peptide filaments appear to be highly specific and inhibited by reducing conditions.

The morphology of the twisted ribbons formed by $A\beta_{(1-28)}$ alone, as reported here, differs somewhat from that reported in the literature and may be due to differences in the types of negative stain used. Gorevic et al. (24) observed $A\beta_{(1-28)}$ peptide fibrils approximately 10 nm in diameter by electron microscopy of uranyl acetate-stained material. In their hands, $A\beta_{(16-28)}$ or $A\beta_{(18-28)}$ formed ribbon-like structures, while $A\beta_{(1-28)}$ did not. Previous negative staining electron microscopy studies did not reveal striations or strands in $A\beta$ peptide fibrils (22–25). We observed double, triple, and multistranded ribbons characterized by longitudinal parallel striations in the $A\beta_{(1-28)}$ fibrils generated in the absence of apoE. Monofibrils formed from $A\beta$ coincubated with apoE3 or apoE4 were 6–7 nm wide. The 8–10 nm $A\beta$ fibrils described in the literature, identified using uranyl acetate negative staining, may reflect single strands that have become physically separated as monofibrils during the staining procedure. This hypothesis is corroborated by the observation that sheet-like structures can be seen upon uranyl acetate staining only with longer peptides (39 amino acids and longer), which aggregate avidly by hydrophobic interactions from the extended hydrophobic transmembrane domain of amyloid precursor protein and might, therefore, resist separating during staining. The twisted ribbon and multistranded sheets of $A\beta$ peptide appear to be stable in silicotungstic acid negative stain (pH 7). The progressive development of multistranded sheets over the 7-d time-course studies suggests that these structures actually exist in the incubations and are not artifacts of the negative staining procedure. Although $A\beta_{(1-28)}$ optimally forms monofibrils at pH 5 (25), which is closer to the pH of uranyl acetate negative stains, we chose silicotungstate at neutrality, which is close to the more physiologic pH used for the incubations.

We have demonstrated that apoE and $A\beta$ peptide incubated together associate to form monofibrils; however, the molecular arrangement of the $A\beta$ peptide and apoE is unclear. Either apoE/$A\beta$ complexes have polymerized to form the monofibrils, or apoE has dissociated any preexisting $A\beta$ multistranded ribbons by strong interactions at specific sites. Further experiments aimed at understanding the mechanism of monofibril generation by apoE are under way.

The relationship of the apoE/$A\beta$ fibrils formed in vitro to the amyloid fibrils of AD senile plaques is not known. However, we think that we have demonstrated a relevant morphological correlate of the known association of $A\beta$ peptide and apoE, two major components of senile plaque. The amount of amyloid peptide deposited in the brains of patients homozygous for apoE4 is greater than that deposited in patients homozygous for apoE3 (19). We report here that apoE4 is more efficient at generating monofibrils with $A\beta$ peptide than apoE3, a further in vitro morphological finding consistent with pathologic and genetic data. The presence of apoE in the senile plaque and the formation of congophilic apoE/$A\beta$ fibrils in vitro may indicate a role for apoE in the mechanism of senile plaque formation. These observations in situ, as well as the isoform-specific interactions of apoE with $A\beta$ at both the molecular and structural level in vitro, suggest that apoE participation is important in the formation and deposition of the extracellular amyloid fibrils characteristic of Alzheimer's disease.

References

1. Selkoe, D. J. 1991. The molecular pathology of Alzheimer's disease. *Neuron.* 6:487–498.

2. Namba, Y., M. Tomonaga, H. Kawasaki, E. Otomo, and K. Ikeda. 1991. Apolipoprotein E immunoreactivity in cerebral amyloid deposits and neurofibrillary tangles in Alzheimer's disease and kuru plaque amyloid in Creutzfeldt–Jakob disease. *Brain Res.* 541:163–166.

3. Wisniewski, T., and B. Frangione. 1992. Apolipoprotein E: a pathological chaperone protein in patients with cerebral and systemic amyloid. *Neurosci. Lett.* 135:235–238.

4. Strittmatter, W. J., A. M. Saunders, D. Schmechel, M. Pericak-Vance, J. Enghild, G. S. Salvesen, and A. D. Roses. 1993. Apolipoprotein E: high avidity binding to β-amyloid and increased frequency of type 4 allele in late-onset familial Alzheimer's disease. *Proc. Natl. Acad. Sci. USA.* 90:1977–1981.

5. Beyreuther, K., and C. L. Masters. 1991. Amyloid precursor protein (APP) and βA4 amyloid in the etiology of Alzheimer's disease: precursor–product relationships in the derangement of neuronal function. *Brain Pathol.* 1:241–251.

6. Ghiso, J., E. Matsubara, A. Koudinov, N. H. Choi-Miura, M. Tomita, T. Wisniewski, and B. Frangione. 1993. The cerebrospinal-fluid soluble form of Alzheimer's amyloid beta is complexed to SP-40,40 (apolipoprotein J), an inhibitor of the complement membrane-attack complex. *Biochem. J.* 293:27–30.

7. Mahley, R. W. 1988. Apolipoprotein E: cholesterol transport protein with expanding role in cell biology. *Science (Wash. DC).* 240:622–630.

8. Boyles, J. K., R. E. Pitas, E. Wilson, R. W. Mahley, and J. M. Taylor. 1985. Apolipoprotein E associated with astrocytic glia of the central nervous system and with nonmyelinating glia of the peripheral nervous system. *J. Clin. Invest.* 76:1501–1513.

9. Pitas, R. E., J. K. Boyles, S. H. Lee, D. Foss, and R. W. Mahley. 1987. Astrocytes synthesize apolipoprotein E and metabolize apolipoprotein E-containing lipoproteins. *Biochim. Biophys. Acta.* 917:148–161.

10. Pitas, R. E., J. K. Boyles, S. H. Lee, D. Y. Hui, and K. H. Weisgraber. 1987. Lipoproteins and their receptors in the central nervous system: characterization of the lipoproteins in cerebrospinal fluid and identification of apolipoprotein B,E(LDL) receptors in the brain. *J. Biol. Chem.* 262:14352–14360.

11. Ignatius, M. J., P. J. Gebicke-Härter, J. H. P. Skene, J. W. Schilling, K. H. Weisgraber, R. W. Mahley, and E. M. Shooter. 1986. Expression of apolipoprotein E during nerve degeneration and regeneration. *Proc. Natl. Acad. Sci. USA.* 83:1125–1129.

12. Ignatius, M. J., E. M. Shooter, R. E. Pitas, and R. W. Mahley. 1987. Lipoprotein uptake by neuronal growth cones in vitro. *Science (Wash. DC).* 236:959–962.

13. Boyles, J. K., C. D. Zoellner, L. J. Anderson, L. M. Kosik, R. E. Pitas, K. H. Weisgraber, D. Y. Hui, R. W. Mahley, P. J. Gebicke-Haerter, M. J. Ignatius, and E. M. Shooter. 1989. A role for apolipoprotein E, apolipoprotein A-I, and low density lipoprotein receptors in cholesterol transport during regeneration and remyelination of the rat sciatic nerve. *J. Clin. Invest.* 83:1015–1031.

14. Snipes, G. J., C. B. McGuire, J. J. Norden, and J. A. Freeman. 1986. Nerve injury stimulates the secretion of apolipoprotein E by nonneuronal cells. *Proc. Natl. Acad. Sci. USA.* 83:1130–1134.

15. Handelmann, G. E., J. K. Boyles, K. H. Weisgraber, R. W. Mahley, and R. E. Pitas. 1992. Effects of apolipoprotein E, β-very low density lipoproteins, and cholesterol on the extension of neurites by rabbit dorsal root ganglion neurons in vitro. *J. Lipid Res.* 33:1677–1688.

16. Nathan, B. P., S. Bellosta, D. A. Sanan, K. H. Weisgraber, R. W. Mahley, and R. E. Pitas. 1994. Differential effects of apolipoproteins E3 and E4 on neuronal growth in vitro. *Science (Wash. DC).* 264:850–852.

17. Saunders, A. M., W. J. Strittmatter, D. Schmechel, P. H. St. George-Hyslop, M. A. Pericak-Vance, S. H. Joo, B. L. Rosi, J. F. Gusella, D. R. Crapper-MacLachlan, M. J. Alberts, C. Hulette, B. Crain, D. Goldgaber, and A. D. Roses. 1993. Association of apolipoprotein E allele ϵ4 with late-onset familial and sporadic Alzheimer's disease. *Neurology.* 43:1467–1472.

18. Corder, E. H., A. M. Saunders, W. J. Strittmatter, D. E. Schmechel, P. C. Gaskell, G. W. Small, A. D. Roses, J. L. Haines, and M. A. Pericak-Vance. 1993. Gene dose of apolipoprotein E type 4 allele and the risk of Alzheimer's disease in late onset families. *Science (Wash. DC).* 261:921–923.

19. Schmechel, D. E., A. M. Saunders, W. J. Strittmatter, B. J. Crain, C. M. Hulette, S. H. Joo, M. A. Pericak-Vance, D. Goldgaber, and A. D. Roses. 1993. Increased amyloid β-peptide deposition in cerebral cortex as a consequence of apolipoprotein E genotype in late-onset Alzheimer's disease. *Proc. Natl. Acad. Sci. USA.* 90:9649–9653.

20. Strittmatter, W. J., K. H. Weisgraber, D. Y. Huang, L.-M. Dong, G. S. Salvesen, M. Pericak-Vance, D. Schmechel, A. M. Saunders, D. Goldgaber, and A. D. Roses. 1993. Binding of human apolipoprotein E to synthetic amyloid β peptide: isoform-specific effects and implications for late-onset Alzheimer's disease. *Proc. Natl. Acad. Sci. USA.* 90:8098–8102.

21. Rall, S. C., Jr., K. H. Weisgraber, and R. W. Mahley. 1986. Isolation and characterization of apolipoprotein E. *Methods Enzymol.* 128:273–287.

22. Castaño, E. M., J. Ghiso, F. Prelli, P. D. Gorevic, A. Migheli, and B. Frangione. 1986. In vitro formation of amyloid fibrils from two synthetic peptides of different lengths homologous to Alzheimer's disease β-protein. *Biochem. Biophys. Res. Commun.* 141:782–789.

23. Kirschner, D. A., H. Inouye, L. K. Duffy, A. Sinclair, M. Lind, and D. J. Selkoe. 1987. Synthetic peptide homologous to β protein from Alzheimer's disease forms amyloid-like fibrils in vitro. *Proc. Natl. Acad. Sci. USA.* 84:6953–6957.

24. Gorevic, P. D., E. M. Castano, R. Sarma, and B. Frangione. 1987. Ten to fourteen residue peptides of Alzheimer's disease protein are sufficient for amyloid fibril formation and its characteristic Xray diffraction pattern. *Biochem. Biophys. Res. Commun.* 147:854–862.

25. Burdick, D., B. Soreghan, M. Kwon, J. Kosmoski, M. Knauer, A. Henschen, J. Yates, C. Cotman, and C. Glabe. 1992. Assembly and aggregation properties of synthetic Alzheimer's A4/β amyloid peptide analogs. *J. Biol. Chem.* 267:546–554.